23rd ABCM International Congress of Mechanical Engineering
December 6-11, 2015, Rio de Janeiro, RJ, Brazil

Decentralized Model Predictive Control of a Formation of Multirotor Helicopters

Ícaro Bezerra Viana
Igor Afonso Acampora Prado
Davi Ferreira de Castro
Davi Antônio dos Santos
Luiz Carlos Sandoval Góes
Instituto Tecnológico de Aeronáutica, Sao José dos Campos, Brazil 12228-900
icaro@ita.br
igorap@ita.br
davifc@ita.br
davists@ita.br
goes@ita.br

Abstract. *This paper treat the problem of position formation flight control of a group of n multirotor helicopters under obstacle and collision avoidance constraints. In order to solve the problem, a decentralized architecture with model predictive controllers (MPC) per vehicle includes a set of convex constraints on the vehicles's position to prevent collisions with other vehicles and obstacles. The resulting decentralized scheme controls the formation based on a virtual structure approach. The performance of the method is assessed through simulations considering that the vehicles is subject to disturbance forces and the results show the effectivenes and the ability of the control architecture to handle the obstacle and collision avoidance constraints.*

Keywords: *aerial robotics, multirotor helicopters, model predictive control, obstacle avoidance, collision avoidance*

1. INTRODUCTION

Formation control of multiple autonomous vehicles has received in the last decade an increasing interest in the control community. Works in this area are generally inspired by the recent results in the coordinated control of multi-agent systems Ailon and Arogeti (2013). Many interesting applications of formation control have been studied. Examples include military and civilian applications such as intelligence, reconnaissance, surveillance, exploration of dangerous environments where Unmanned Aerial Vehicles (UAVs) can replace humans. In the context of obstacle avoidance with UAV of multirotor type, it is indispensable that the multirotor helicopter have incorporated this ability. This capacity can be used in the exploration of product delivering, because obstacles can not be pictured in a satellite view of the delivery site.

Main considerations in formation flying include how to come together and maintain a formation and how to achieve collision/obstacle avoidance. The phrase "collision avoidance" is used to refer to a UAV trying to avoid another UAV, and the expression "obstacle avoidance" represents the scenario where the UAVs try to avoid obstacles. To ensure collision avoidance Schouwenaars *et al.* (2006) uses an approach called mixed integer linear programming (MILP) for the trajectory planning of multiple UAVs, where integer variables are added to the optimization process in order to deal with the constraints properly. Additionally, Kuwata and How (2003) also used MILP, in this case to design dynamically feasible trajectories for obstacle avoidance.

This paper presents a control system for flight in formation of multiple autonomous multirotors helicopters, adopting a virtual structure configuration. In this, guiding the group of vehicles is easier than in other configurations, since all the agents of the formation are treated as a single object (Chao *et al.* 2011). In order to ensure, simultaneously, performance in the trajectory tracking and treating the obstacle and collision avoidance constraints between vehicles, a structure with MPC controllers is used for guiding the vehicles. In this, the design of a position controller is replicated for each vehicle that composed the formation, consisting of a linear state-space model predictive control (MPC) strategy. This paper extends the trajectory control problem presented earlier in Prado and Santos (2013) and Santos *et al.* (2013), including integer constraints on the problem formulation using a quadratic cost function, resulting in a MIQP (mixed-integer quadratic program). The main contribution of this paper is the incorporation of a MIQP form in a predictive control scheme to treat the obstacle/collision avoidance problem for multirotor helicopters.

Figure 1 shows the block diagram with the architecture composed of three model predictive controllers (MPC) to the formation control, where each controller is capable to controlling only the three-dimensional position $r^{(i)} \in \mathbb{R}^3$ of a multirotor helicopter to follow a time-varying position command $\bar{r}^{(i)} \in \mathbb{R}^3$, where i denotes the i^{th} vehicle. To implement the set of constraints in the MPC, we assume that needed information can be measured and communicated in real time, so that each vehicle position information is passed on to neighboring vehicles of the formation. The variable $\bar{\rho}_{(ij)}$ are the increment for the desired position of the vehicle j in relation to the vehicle i, $\forall i \neq j$.

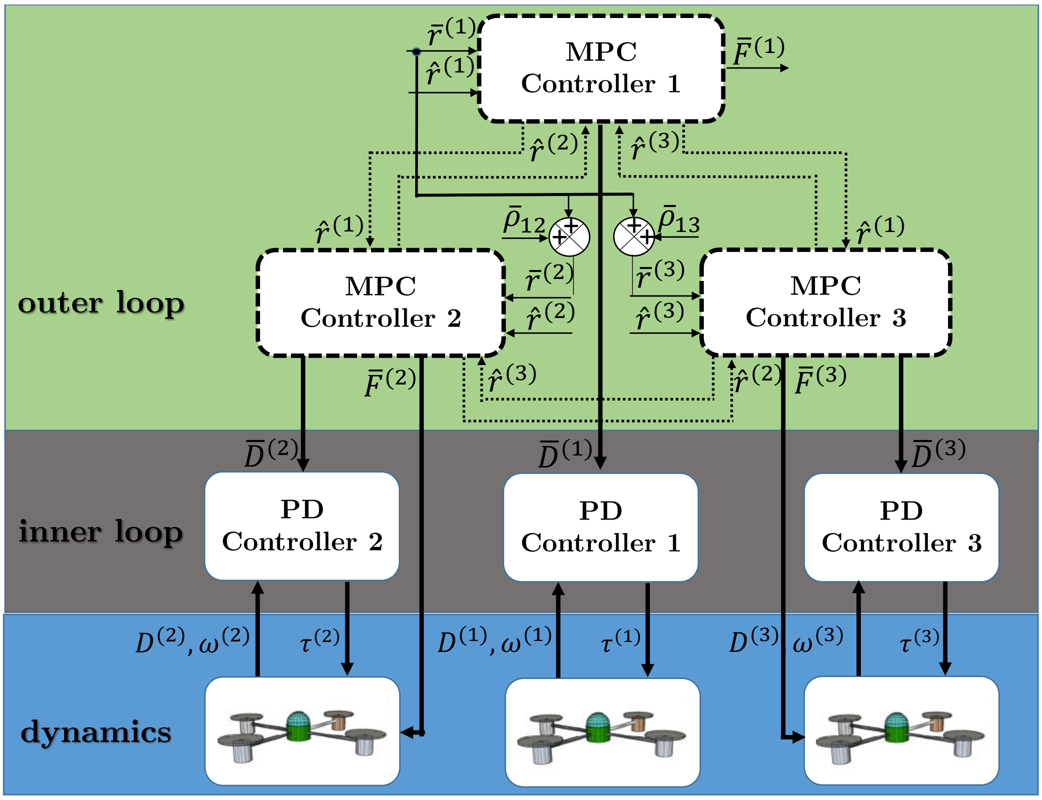

Figure 1. Block diagram of a formation flight control for three multirotors.

The control system for each multirotor is composed of an outer loop represented by the MPC for position control, and a inner loop for attitude control. The Attitude Control block receives an attitude command $\bar{D} \in \mathrm{SO}(3)$ and produces the control torque $\boldsymbol{\tau} \in \mathbb{R}^3$ to incline the rotor plane with respect to the horizontal plane. The outer loop has the role of generating the throttle command (command for the total thrust magnitude) $\bar{F} \in \mathbb{R}$ and the attitude command $\bar{D}$ necessary to accelerate the multirotor in such a way to control its position as desired. These commands are generated by the outer loop of the system after the conversion of the control vector computed by the MPC.

The rest of the body text is organized as follows: Section II presents the definition of the problem. Section III describes the problem solution. Section IV describes the evaluation based on computer simulations using MATLAB/SIMULINK and Section V contains the conclusions and suggestions for future works.

2. PROBLEM STATEMENT

Consider the multirotor vehicle and the three Cartesian coordinate systems (CCS) illustrated in Figure 2. It is assumed that the vehicle has a rigid structure. The body CCS $S_{\mathrm{B}} \triangleq \{X_{\mathrm{B}}, Y_{\mathrm{B}}, Z_{\mathrm{B}}\}$ is fixed to the structure and its origin coincides with the center of mass (CM) of the vehicle. The reference CCS $S_{\mathrm{R}} \triangleq \{X_{\mathrm{R}}, Y_{\mathrm{R}}, Z_{\mathrm{R}}\}$ is Earth-fixed and its origin is at point O. Finally, the CCS $S_{\mathrm{R'}} \triangleq \{X_{\mathrm{R'}}, Y_{\mathrm{R'}}, Z_{\mathrm{R'}}\}$ is defined to be parallel to S_{R}, but its origin is shifted to CM. Assume that S_{R} is an inertial frame.

Invoking the second Newton's law and neglecting disturbance forces, the translational dynamics of the multirotor illustrated in Figure 2 can be immediately described in S_{R} by the following second order differential equation:

$$\ddot{\mathbf{r}} = \frac{1}{m}\mathbf{f} + \begin{bmatrix} 0 \\ 0 \\ -g \end{bmatrix}, \tag{1}$$

where $\mathbf{r} \triangleq [r_{\mathrm{x}}\ r_{\mathrm{y}}\ r_{\mathrm{z}}]^{\mathrm{T}} \in \mathbb{R}^3$ is the position vector of CM, $\mathbf{f} \triangleq [f_{\mathrm{x}}\ f_{\mathrm{y}}\ f_{\mathrm{z}}]^{\mathrm{T}} \in \mathbb{R}^3$ is the total thrust vector, m is the mass of the vehicle, and g is the gravitational acceleration. As illustrated in Figure 2, $\mathbf{f}$ is perpendicular to the rotor plane.

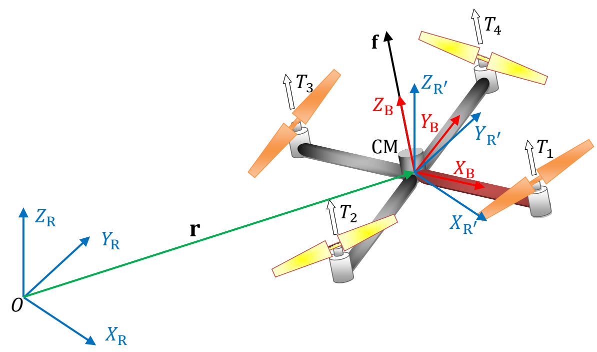

Figure 2. The Cartesian coordinate systems.

Define the inclination angle $\phi \in \mathbb{R}$ of the rotor plane as the angle between Z_{B} and $Z_{\mathrm{R'}}$. The angle ϕ can thus be expressed by

$$\phi \triangleq \cos^{-1}\frac{f_{\mathrm{z}}}{f}, \tag{2}$$

where $f \triangleq \|\mathbf{f}\|$.

Define the position tracking error $\tilde{\mathbf{r}} \in \mathbb{R}^3$ as

$$\tilde{\mathbf{r}} \triangleq \mathbf{r} - \mathbf{r}_{\mathrm{d}}, \tag{3}$$

where $\mathbf{r}_{\mathrm{d}} \triangleq [r_{\mathrm{d,x}}\ r_{\mathrm{d,y}}\ r_{\mathrm{d,z}}]^{\mathrm{T}} \in \mathbb{R}^3$ is a position command.

Problem 1. Let $\phi_{\max} \in \mathbb{R}$ denote the maximum allowable value of ϕ, $f_{\min} \in \mathbb{R}$ and $f_{\max} \in \mathbb{R}$ denote, respectively, the minimum and maximum allowable values of f, and $\mathbf{r}_{\min} \in \mathbb{R}^3$ and $\mathbf{r}_{\max} \in \mathbb{R}^3$ denote, respectively, the minimum and maximum allowable values of $\mathbf{r}$. The problem is to find a control law for $\mathbf{f}$ that minimizes $\tilde{\mathbf{r}}$, subject to the inclination constraint $\phi \leq \phi_{\max}$, to the force magnitude constraint $f_{\min} \leq f \leq f_{\max}$, and to the position constraint $\mathbf{r}_{\min} \leq \mathbf{r} \leq \mathbf{r}_{\max}$.

Problem 2. Let $\mathbf{L}^l \in \mathbb{R}^3$ and $\mathbf{U}^l \in \mathbb{R}^3$ denote, respectively, the coordinates of the lower left-hand corner and the upper right-hand corner of a static obstacle l. The problem consists in include avoidance requirements so that a control action should calculate a command $\mathbf{f}^{(i)}$ by ensuring that the current position of the ith vehicle $\mathbf{r}^{(i)}$ lie outside the obstacle l, at each time step, as show in Figure 1.

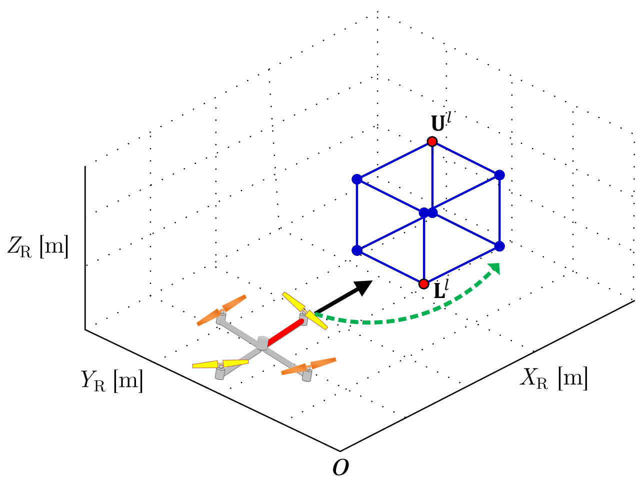

Figure 3. Obstacle avoidance problem

The obstacles can be modeled in this framework as convex polygons of any number of sides, but, to simplify the presentation, the results in this paper only use cubes, as shows in Figure 3. It is assumed that the location of the cube obstacle defined by $\mathbf{L}^l$ and $\mathbf{U}^l$ are known. Thus, to achieve the obstacle avoidance and to attend the requirement proposed simply add the following set of linear inequality convex constraints in the problem formulation,

$$r_x^{(i)} \leq L_x^{(l)} \tag{4}$$

$$or,\ r_x^{(i)} \geq U_x^{(l)} \tag{5}$$

$$r_y^{(i)} \leq L_y^{(l)} \tag{6}$$

$$or,\ r_y^{(i)} \geq U_y^{(l)} \tag{7}$$

$$r_z^{(i)} \leq L_z^{(l)} \tag{8}$$

$$or,\ r_z^{(i)} \geq U_z^{(l)} \tag{9}$$

where $\mathbf{r}^{(i)}$ is the manipulated variable of the optimization process that integrates the MPC controller. These constraints can be represented by the following mixed-integer form by introducing binary variables Williams and Brailsford (1996):

$$r_x^{(i)} \leq L_x^{(l)} + Ma_1^{(il)} \tag{10}$$

$$and,\ -r_x^{(i)} \leq -U_x^{(l)} + Ma_2^{(il)} \tag{11}$$

$$r_y^{(i)} \leq L_y^{(l)} + Ma_3^{(il)} \tag{12}$$

$$and,\ -r_y^{(i)} \leq -U_y^{(l)} + Ma_4^{(il)} \tag{13}$$

$$r_z^{(i)} \leq L_z^{(l)} + Ma_5^{(il)} \tag{14}$$

$$and,\ -r_z^{(i)} \leq -U_z^{(l)} + Ma_6^{(il)} \tag{15}$$

$$and, \quad \sum_{p=1}^{6} a_p \leq 5 \tag{16}$$

A set of binary variables a_p was added to the problem at each time step. The variable M denote an arbitrary positive number, larger than any distance in the problem. This process can be extended to a general number of time steps, vehicles and obstacles, considering the number of dimensions $N = 3$ and n equal to x, y, or z. The binary variables $a_p^{(il)}$ are the switches, with $p \in [1, ..., 2N]$, corresponding to being on one two sides of the obstacle in each of N dimensions. The complete formulation is,

$$\forall i, \forall l, \forall k \in [1, ..., T-1]: \quad r_n^{(i)}(k) \geq U_n^l - Ma_n^{(il)}(k), \quad \forall n \tag{17}$$

$$and, \qquad r_n^{(i)}(k) \leq L_n^l - Ma_{n+N}^{(il)}(k), \quad \forall n \tag{18}$$

$$and, \quad \sum_{p=1}^{2N} b_a^{(il)}(k) \leq 2N - 1 \tag{19}$$

The new constraints in (17-19) are linear in the decision variables, and so the new problem is a MIQP.

Problem 3. Let a standalone controller referring to a i^{th} vehicle of the formation, a control action should calculate a command $\mathbf{f}^{(i)}$ so that $\mathbf{r}^{(i)}$, the current position of the vehicle (i), stay at a safety distance $\mathbf{D} \triangleq [d_\mathrm{x}\ d_\mathrm{y}\ d_\mathrm{z}]^\mathrm{T} \in \mathbb{R}^3$ in relation to $\mathbf{r}^{(j)}, \forall j \neq i$ at each time step, as show in Figure 4.

In Figure 4 the variable l corresponds to the protection sphere radius of each vehicle and d_{ij} corresponds to the safety distances represented in the three-dimensional space. Thus, to ensure that these spheres do not collide, the minimum distance d_{ij} should be at least twice the sphere radius, where the value of l can be specified as the sum of the distance of the center of mass (CM) in relation to the rotor center, plus the length of the radius propeller. This corresponds to the enforcement of a rectangular exclusion region around each vehicle.

It is assumed that, at each instant of time k, the multirotor (i) can get the information of vehicle position (j). Thus, to achieve the collision avoidance simply add the following set of linear inequality convex constraints,

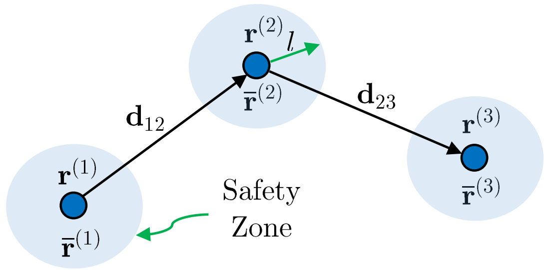

Figure 4. Collision avoidance problem

$$r_x^{(i)} - \hat{r}_x^{(j)} \geq d_{x_{ij}} \tag{20}$$

$$or,\ \hat{r}_x^{(j)} - r_x^{(i)} \geq d_{x_{ij}} \tag{21}$$

$$r_y^{(i)} - \hat{r}_y^{(j)} \geq d_{y_{ij}} \tag{22}$$

$$or,\ \hat{r}_y^{(j)} - r_y^{(i)} \geq d_{y_{ij}} \tag{23}$$

$$r_z^{(i)} - \hat{r}_z^{(j)} \geq d_{z_{ij}} \tag{24}$$

$$or,\ \hat{r}_z^{(j)} - r_z^{(i)} \geq d_{z_{ij}} \tag{25}$$

where $\mathbf{r}^{(i)}$ is the manipulated variable of the optimization process that integrates the MPC controller. As in the preceding problem, these can be converted to the more useful *and* constraints by introducing binary variables, giving

$$r_x^{(i)} - \hat{r}_x^{(j)} \geq d_{x_{ij}} - Mb_1^{(ij)} \tag{26}$$

$$and,\ \hat{r}_x^{(j)} - r_x^{(i)} \geq d_{x_{ij}} - Mb_2^{(ij)} \tag{27}$$

$$r_y^{(i)} - \hat{r}_y^{(j)} \geq d_{y_{ij}} - Mb_3^{(ij)} \tag{28}$$

$$and,\ \hat{r}_y^{(j)} - r_y^{(i)} \geq d_{y_{ij}} - Mb_4^{(ij)} \tag{29}$$

$$r_z^{(i)} - \hat{r}_z^{(j)} \geq d_{z_{ij}} - Mb_5^{(ij)} \tag{30}$$

$$and,\ \hat{r}_z^{(j)} - r_z^{(i)} \geq d_{z_{ij}} - Mb_6^{(ij)} \tag{31}$$

$$and, \quad \sum_{p=1}^{6} b_p \leq 5 \tag{32}$$

where b_p is the binary variables added to the problem and M is the same large number used in the preceding section.

This is extended to the general case using the same notation as before. The safety avoidance distance in direction n is d_n. The condition $j > i$ avoids duplication of the constraints on the positions of pairs of vehicles. The complete formulation is,

$$\forall i, j | j > i, \forall k \in [1, ..., T-1] : \quad r_n^{(i)}(k) - \hat{r}_n^{(j)}(k) \geq d_n - Mb_n^{(ij)}(k), \quad \forall n \tag{33}$$

$$and, \qquad \hat{r}_n^{(j)}(k) - r_n^{(i)}(k) \geq d_n - Mb_{n+N}^{(il)}(k), \quad \forall n \tag{34}$$

$$and, \qquad \sum_{p=1}^{2N} b_p^{(ij)}(k) \leq 2N - 1 \tag{35}$$

3. Problem Solution

The solution to Problem 1 is based on a MPC strategy, described in more details in Prado and Santos (2013). In short, the Problem 1 is solved using a linear state-space model predictive control whose optimization is made handy by replacing the original conic constraint set on the thrust vector by an inscribed pyramidal space, which rendered a linear set of inequalities. This section proposes a solution to the Problem 2 and 3 by inserting linear convex constraints to the optimization problem. Subsection 3.1 describes the system by a discrete-time linear state-space model in the form of incremental control input.

3.1 Incremental-Input State-Space Model

Define the state vector $\mathbf{x} \triangleq [r_{\mathrm{x}}\ \dot{r}_{\mathrm{x}}\ r_{\mathrm{y}}\ \dot{r}_{\mathrm{y}}\ r_{\mathrm{z}}\ \dot{r}_{\mathrm{z}}]^{\mathrm{T}} \in \mathbb{R}^6$ and the control input vector $\mathbf{u} \triangleq [u_{\mathrm{x}}\ u_{\mathrm{y}}\ u_{\mathrm{z}}]^{\mathrm{T}} \in \mathbb{R}^3$

$$\mathbf{u} \triangleq \frac{1}{m}\mathbf{f} - \begin{bmatrix} 0 \\ 0 \\ g \end{bmatrix}. \tag{36}$$

Using equation (36), (1) can be immediately rewritten as a continuous-time linear state-space model

$$\dot{\mathbf{x}} = \mathbf{A}\mathbf{x} + \mathbf{B}\mathbf{u}, \tag{37}$$

with

$$\mathbf{A} = \begin{bmatrix} 0 & 1 & 0 & 0 & 0 & 0 \\ 0 & 0 & 0 & 0 & 0 & 0 \\ 0 & 0 & 0 & 1 & 0 & 0 \\ 0 & 0 & 0 & 0 & 0 & 0 \\ 0 & 0 & 0 & 0 & 0 & 1 \\ 0 & 0 & 0 & 0 & 0 & 0 \end{bmatrix} \in \mathbb{R}^{6\times 6} \tag{38}$$

and

$$\mathbf{B} = \begin{bmatrix} 0 & 0 & 0 \\ 1 & 0 & 0 \\ 0 & 0 & 0 \\ 0 & 1 & 0 \\ 0 & 0 & 0 \\ 0 & 0 & 1 \end{bmatrix} \in \mathbb{R}^{6\times 3}. \tag{39}$$

Define the controlled output vector $\mathbf{y} \in \mathbb{R}^3$ to be the position vector, i.e.

$$\mathbf{y} \triangleq \mathbf{C}\mathbf{x}, \tag{40}$$

with

$$\mathbf{C} = \begin{bmatrix} 1 & 0 & 0 & 0 & 0 & 0 \\ 0 & 0 & 1 & 0 & 0 & 0 \\ 0 & 0 & 0 & 0 & 1 & 0 \end{bmatrix} \in \mathbb{R}^{3\times 6}. \tag{41}$$

Let $\mathbf{x}(k) \in \mathbb{R}^6$, $\mathbf{u}(k) \in \mathbb{R}^3$, and $\mathbf{y}(k) \in \mathbb{R}^3$ denote, respectively, the state vector, the control input vector and the controlled output vector, all described in the discrete-time domain. Using the Euler integration method with an integration step of $T_s = 20$ ms, the discretized version of equation (37) and (40) is obtained as

$$\begin{array}{lcl} \mathbf{x}(k+1) & = & \mathbf{A}_{\mathrm{d}}\mathbf{x}(k) + \mathbf{B}_{\mathrm{d}}\mathbf{u}(k) \\ \mathbf{y}(k) & = & \mathbf{C}_{\mathrm{d}}\mathbf{x}(k) \end{array}, \tag{42}$$

where

$$\mathbf{A}_{\mathrm{d}} = \begin{bmatrix} 1 & 0.02 & 0 & 0 & 0 & 0 \\ 0 & 1 & 0 & 0 & 0 & 0 \\ 0 & 0 & 1 & 0.02 & 0 & 0 \\ 0 & 0 & 0 & 1 & 0 & 0 \\ 0 & 0 & 0 & 0 & 1 & 0.02 \\ 0 & 0 & 0 & 0 & 0 & 1 \end{bmatrix} \in \mathbb{R}^{6\times 6}, \tag{43}$$

$$\mathbf{B}_{\mathrm{d}} = \begin{bmatrix} 0.0002 & 0 & 0 \\ 0.02 & 0 & 0 \\ 0 & 0.0002 & 0 \\ 0 & 0.02 & 0 \\ 0 & 0 & 0.0002 \\ 0 & 0 & 0.02 \end{bmatrix} \in \mathbb{R}^{6\times 3}, \tag{44}$$

and $\mathbf{C}_{\mathrm{d}} \in \mathbb{R}^{3\times 6}$ remains equal to $\mathbf{C}$.

Consider the discrete-time state-space model of equation (42). It can be rewritten in the incremental-input form as Maciejowski (2002),

$$\begin{array}{lcl} \boldsymbol{\xi}(k+1) & = & \tilde{\mathbf{A}}\boldsymbol{\xi}(k) + \tilde{\mathbf{B}}\Delta\mathbf{u}(k) \\ \mathbf{y}(k) & = & \tilde{\mathbf{C}}\boldsymbol{\xi}(k) \end{array}, \tag{45}$$

with

$$\boldsymbol{\xi}(k) = \begin{bmatrix} \Delta\mathbf{x}(k) \\ \mathbf{y}(k) \end{bmatrix} \in \mathbb{R}^{9}, \tag{46}$$

$$\tilde{\mathbf{A}} = \begin{bmatrix} \mathbf{A}_{\mathrm{d}} & \mathbf{0}_{6\times 3} \\ \mathbf{C}_{\mathrm{d}}\mathbf{A}_{\mathrm{d}} & \mathbf{I}_3 \end{bmatrix} \in \mathbb{R}^{9\times 9}, \tag{47}$$

$$\tilde{\mathbf{B}} = \begin{bmatrix} \mathbf{B}_{\mathrm{d}} \\ \mathbf{C}_{\mathrm{d}}\mathbf{B}_{\mathrm{d}} \end{bmatrix} \in \mathbb{R}^{9\times 3}, \tag{48}$$

and

$$\tilde{\mathbf{C}} = \begin{bmatrix} \mathbf{0}_{3\times 6} & \mathbf{I}_3 \end{bmatrix} \in \mathbb{R}^{3\times 9}, \tag{49}$$

where $\Delta\mathbf{x}(k) \triangleq \mathbf{x}(k) - \mathbf{x}(k-1) \in \mathbb{R}^6$ denotes the incremental state vector, $\Delta\mathbf{u}(k) \triangleq \mathbf{u}(k) - \mathbf{u}(k-1) \in \mathbb{R}^3$ is the incremental control input vector, $\mathbf{I}_3$ represents an identity matrix with dimensions 3×3, and $\mathbf{0}_{3\times 6}$ is a matrix of zeros with dimension 3×6.

3.2 Prediction Model

Using equation (45), the prediction model can be obtained as (see Maciejowski (2002), p.50)

$$\hat{\mathbf{y}}_N = \mathbf{G}\Delta\hat{\mathbf{u}}_M + \mathbf{F}, \tag{50}$$

where $\hat{\mathbf{y}}_N \in \mathbb{R}^{3N\times 1}$ stacks the controlled outputs along a prediction horizon of length N, $\Delta\hat{\mathbf{u}}_M \in \mathbb{R}^{3M\times 1}$ stacks the incremental control inputs along a control horizon of length M,

$$\mathbf{G} = \begin{bmatrix} \tilde{\mathbf{C}}\tilde{\mathbf{B}} & \mathbf{0}_{3\times 3} & \dots & \mathbf{0}_{3\times 3} \\ \tilde{\mathbf{C}}\tilde{\mathbf{A}}\tilde{\mathbf{B}} & \tilde{\mathbf{C}}\tilde{\mathbf{B}} & \dots & \mathbf{0}_{3\times 3} \\ \vdots & \vdots & \ddots & \vdots \\ \tilde{\mathbf{C}}\tilde{\mathbf{A}}^{M-1}\tilde{\mathbf{B}} & \tilde{\mathbf{C}}\tilde{\mathbf{A}}^{M-2}\tilde{\mathbf{B}} & \dots & \tilde{\mathbf{C}}\tilde{\mathbf{B}} \\ \vdots & \vdots & & \vdots \\ \tilde{\mathbf{C}}\tilde{\mathbf{A}}^{N-1}\tilde{\mathbf{B}} & \tilde{\mathbf{C}}\tilde{\mathbf{A}}^{N-2}\tilde{\mathbf{B}} & \dots & \tilde{\mathbf{C}}\tilde{\mathbf{A}}^{N-M}\tilde{\mathbf{B}} \end{bmatrix} \in \mathbb{R}^{3N\times 3M} \tag{51}$$

and

$$\mathbf{F} = \begin{bmatrix} \tilde{\mathbf{C}}\tilde{\mathbf{A}} \\ \tilde{\mathbf{C}}\tilde{\mathbf{A}}^2 \\ \vdots \\ \tilde{\mathbf{C}}\tilde{\mathbf{A}}^{\mathrm{N}} \end{bmatrix} \boldsymbol{\xi}(k) \in \mathbb{R}^{3N}. \tag{52}$$

3.3 Obstacle Avoidance

Consider the following linear convex inequality constraint in matrix form, according to (4-9),

$$\mathbf{U}^l \leqslant \mathbf{r}^{(i)} \leqslant \mathbf{L}^l \tag{53}$$

The above constraints are employed in this work to avoid that the multirotor (i) collides with the static obstacle (l). The vector $\mathbf{L} \triangleq [{L_x}^{(l)} {L_y}^{(l)} {L_z}^{(l)}]^{\mathrm{T}} \in \mathbb{R}^3$ corresponds to vertex of obstacle with the minimum value of each coordinate of the vehicle. The vector $\mathbf{U} \triangleq [{U_x}^{(l)} {U_y}^{(l)} {U_z}^{(l)}]^{\mathrm{T}} \in \mathbb{R}^3$ corresponds to vertex of obstacle with the maximum value of each coordinate. Repeating equation (53) along the prediction horizon N, yields,

$$[\mathbf{U}^l]_N \leqslant \mathcal{Y}_N \leqslant [\mathbf{L}^l]_N. \tag{54}$$

Replacing the prediction model (50) into equation (54), and rewriting in terms of the optimization vector $\mathcal{X} \in \mathbb{R}^{(3M+n_d N)}$, with n_d the number of binary variables, one can obtain

$$\mathcal{A}\mathcal{X} \leqslant \gamma \tag{55}$$

where,

$$\mathcal{X} \triangleq \left[\begin{array}{cc} \Delta\mathcal{U}_M & a_p^{(il)} \end{array} \right]^{\mathrm{T}}. \tag{56}$$

and,

$$\mathcal{A} \triangleq \left[\begin{array}{ccc} \textbf{-G} & -M\mathbf{I}_{\frac{\mathrm{n_d}}{2}\mathrm{N}} & \mathbf{0}_{\frac{\mathrm{n_d}}{2}\mathrm{N}\times\frac{\mathrm{n_d}}{2}\mathrm{N}} \\ \mathbf{G} & \mathbf{0}_{\frac{\mathrm{n_d}}{2}\mathrm{N}\times\frac{\mathrm{n_d}}{2}\mathrm{N}} & -M\mathbf{I}_{\frac{\mathrm{n_d}}{2}\mathrm{N}} \end{array} \right], \tag{57}$$

where $\mathcal{A} \in \mathbb{R}^{n_d N\times(3M+n_d N)}$ and the scalar M is a larger positive number previously defined. The vector γ is expressed by,

$$\gamma \triangleq \left[\begin{array}{c} \mathbf{F} - [\mathbf{U}^l]_N \\ [\mathbf{L}^l]_N - \mathbf{F} \end{array} \right] \in \mathbb{R}^{n_d N}. \tag{58}$$

which consists in the incremental form of the constraints on the controlled output of the $i^{\acute{th}}$ vehicle. The matrix $\mathcal{A}$ and the vector γ define linear inequality constraints on the optimization variables.

3.4 Collision Avoidance

Consider the following linear convex inequality constraint for the distances between the multirotors in matrix form, according to (20-25),

$$\mathbf{r}^{(i)} - \hat{\mathbf{r}}^{(j)} \geqslant \mathbf{D} \tag{59}$$

The above constraints are employed in this work to avoid collisions between the vehicles (i) and (j), $\forall j \neq i$. The vector $\mathbf{D} \in \mathbb{R}^3$ corresponds to safety distances $d_{x_{ij}}, d_{y_{ij}}, d_{z_{ij}}$ in each direction of the vehicle. Repeating equation (59) along the prediction horizon N, yields,

$$\mathcal{Y}_N - [\hat{\mathbf{r}}^{(j)}]_N \geqslant [\mathbf{D}]_N. \tag{60}$$

Replacing the prediction model (50) into equation (60), and rewriting in terms of the optimization vector $\mathcal{X} \in \mathbb{R}^{(3M+n_d N)}$, with n_d the number of binary variables, one can obtain,

$$\mathcal{A}\mathcal{X} \leqslant \gamma \tag{61}$$

where,

$$\mathcal{X} \triangleq \begin{bmatrix} \Delta\mathcal{U}_M & b_p^{(ij)} \end{bmatrix}^{\mathrm{T}}. \tag{62}$$

and,

$$\mathcal{A} \triangleq \begin{bmatrix} \textbf{-G} & -M\mathbf{I}_{\frac{\mathrm{n_d}}{2}\mathrm{N}} & \mathbf{0}_{\frac{\mathrm{n_d}}{2}\mathrm{N}\times\frac{\mathrm{n_d}}{2}\mathrm{N}} \\ \mathbf{G} & \mathbf{0}_{\frac{\mathrm{n_d}}{2}\mathrm{N}\times\frac{\mathrm{n_d}}{2}\mathrm{N}} & -M\mathbf{I}_{\frac{\mathrm{n_d}}{2}\mathrm{N}} \end{bmatrix}, \tag{63}$$

where $\mathcal{A} \in \mathbb{R}^{n_d N \times (3M+n_d N)}$ and the vector γ is expressed by,

$$\gamma \triangleq \begin{bmatrix} -[\mathbf{D}]_N + \mathbf{F} - [\hat{\mathbf{r}}^{(j)}]_N \\ -[\mathbf{D}]_N + \mathbf{F} + [\hat{\mathbf{r}}^{(j)}]_N \end{bmatrix} \in \mathbb{R}^{n_d N}. \tag{64}$$

3.5 Model Predictive Controller

The optimal control vector $\mathbf{u}^*(k)$ computed at the discrete-time instant k is given by $\mathbf{u}^*(k) = \Delta\mathbf{u}^*(k) + \mathbf{u}^*(k-1)$, where $\Delta\mathbf{u}^*(k)$ is the first control vector of $\Delta\mathbf{u}^*_M$, which in turn is obtained by minimizing the following quadratic cost function:

$$J\left(\Delta\hat{\mathbf{u}}_M\right) = \left(\hat{\mathbf{y}}_N - [\mathbf{r}_{\mathrm{d}}]_N\right)^{\mathrm{T}} \mathbf{Q}\left(\hat{\mathbf{y}}_N - [\mathbf{r}_{\mathrm{d}}]_N\right) + \Delta\hat{\mathbf{u}}_M^{\mathrm{T}}\mathbf{R}\Delta\hat{\mathbf{u}}_M, \tag{65}$$

subject to the constraints (55-61).

In this work, the controlled output weighting matrix is assumed to be $\mathbf{Q} = \boldsymbol{\eta} \times \mathbf{I}_{3N}$ and the control input weighting matrix is assumed to be $\mathbf{R} = \boldsymbol{\rho} \times \mathbf{I}_{3M}$.

3.6 Computing Thrust Magnitude and Attitude Commands

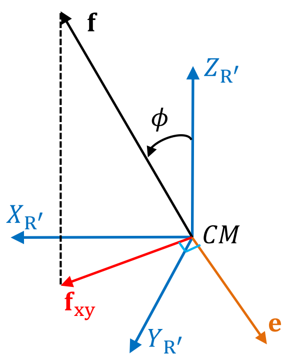

Figure 5. Relation between the thrust vector $\mathbf{f}$ and its horizontal projection $\mathbf{f}_{\mathrm{xy}}$.

In according to Santos (2013), after computation of the control input $\mathbf{u}$, for implementation purposes, it is necessary to transform it into the corresponding commands of total thrust magnitude (throttle) f and attitude.

Rewrite equation (13) as

$$\begin{bmatrix} f_{\mathrm{x}} \\ f_{\mathrm{y}} \\ f_{\mathrm{z}} \end{bmatrix} = m \begin{bmatrix} u_{\mathrm{x}} \\ u_{\mathrm{y}} \\ u_{\mathrm{z}} + g \end{bmatrix}, \tag{66}$$

Table 1. Vehicle Parameters

Variables	Values
Vehicle mass, m	1 kg
Gravitational acceleration, g	9.81 m/s^2
Inertia I_x, I_y	1.71×10^{-2} kg m^2
Inertia I_z	2.86×10^{-2} kg m^2
Thrust factor	3.13×10^{-7}
Torque factor	7.5×10^{-7}
Lenght of arm, l	0.2 m

whose magnitude f is given by

$$f = m\sqrt{u_{\mathrm{x}}^2 + u_{\mathrm{y}}^2 + (u_{\mathrm{z}} + g)^2}, \tag{67}$$

which is the command for the magnitude of the total thrust $\bar{F}$.

The attitude commands $\bar{D}$ for the internal attitude control loop (see Figure 1) need to be computed from vector **f**, which has information about the orientation of the plane of rotors with respect the local horizontal. Note that there are infinite attitudes of S_{B} with respect to $S_{\mathrm{R}'}$ for which the Z_{B} axis coincides with **f**. In order to specify an unique attitude, it is necessary to select a heading angle. For example (since this work is not concerned with heading control), one can choose a zero heading angle, which is equivalent to just taking into consideration the attitude represented by the principal Euler angle/axis $(\phi, \mathbf{e})$, where ϕ is the inclination angle itself and the unit vector **e** (see Figure 5) is given by

$$\mathbf{e} = \frac{Z_{\mathrm{R}'} \times \mathbf{f}_{\mathrm{xy}}}{\| Z_{\mathrm{R}'} \times \mathbf{f}_{\mathrm{xy}} \|}, \tag{68}$$

where $\mathbf{f}_{\mathrm{xy}} \triangleq [f_{\mathrm{x}}\ f_{\mathrm{y}}]^{\mathrm{T}}$ denotes the horizontal projection of **f**. From $(\phi, \mathbf{e})$, this work represent the attitude of S_{B} with respect to S_{R} using direction cosine matrix (DCM) (Shuster (1993)).

4. Simulation Results

In this section, the proposed method is evaluated on the basis of computational simulations by using the MATLAB/SIMULINK software. The environment implemented containing a formation with a group of three multirotors helicopters adopting the Virtual Structure (VS) strategy. The selection of this formation configuration was due to the fact that not provide the error propagation to a neighboring vehicle when a subject vehicle undergoes a disturbance or external interference. The decentralized scheme is composed of three computers connected by a network of Ethernet communication. Each computer contains a MPC controller and the dynamic model of the multirotor helicopter, and sends data via Ethernet of your position $\mathbf{r}^{(i)}$ for the others computers of the architecture. The exchange of position information is necessary in order to achieve the requirements of collision avoidance. Each computer is managed by the operating system Windows 7 Ultimate with Service Pack 1 and runs MATLAB/Simulink version 2012a. Figure 6 summarizes the configuration of the transmit data address used in the network.

The 6DOF dynamics of a multirotor is simulated using the Runge-Kutta 4 as the solver with an integration step of 0.02s. The parameters of the platform is showed in Table I. In order to solve the optimization problem embedded in the MPC algorithm, the branch-and-bound method implemented in the CPLEX software package is taken into account. The following parameterization is adopted for the controller. The control input weights and the controlled output weights are adjusted in $\boldsymbol{\rho} = [0.01\ 0.01\ 0.01]^{\mathrm{T}}$ and $\boldsymbol{\eta} = [1\ 1\ 1]^{\mathrm{T}}$, respectively. The prediction horizon and control horizon are set to $N = 70$ and $M = 5$, respectively. We assumed that the positions of the obstacles are known at each sample. Then, the coordinates of the static obstacle are $\mathbf{L}^{l} = [1.4\ 1.4\ 1.4]^{\mathrm{T}}$ and $\mathbf{U}_{l} = [1.9\ 2.5\ 2.9]^{\mathrm{T}}$. The maximum and minimum constraints on the force magnitude are set in $f_{\max} = 20$ N and $f_{\min} = 2$ N, respectively. Concerning the maximum inclination constraint ϕ_{max} was adopted a value of 30°. The attitude controller are proportional-derivative laws tuned so as to make the attitude dynamics have a bandwidth significantly larger than the bandwidth of the position control dynamics.

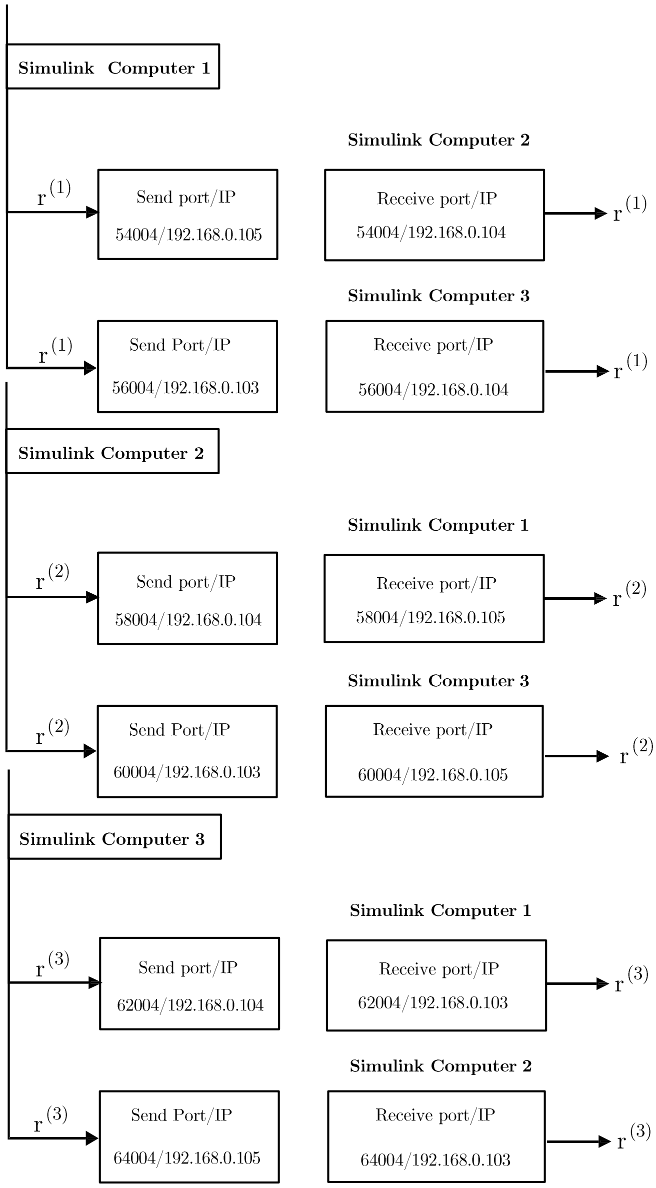

Figure 6. Configuring the sending and receiving of $\mathbf{r}^{(i)}$.

Consider a spiral trajectory parameterized by $r_d(t) = [x_d(t)\ y_d(t)\ z_d(t)]^{\mathrm{T}}$ with $x_d(t) = 2cos(0.2t)$, $y_d(t) = -2sin(0.2t)$ and $z_d(t) = 0.3t + 1$, where $t \geq 0$ denotes the continuous time. The underlying control task is to establish a triangular formation flight of three multirotors. The vehicles leaving the following initial position in meters (m): $\mathbf{r}^{(1)} = [0.5\ 0.5\ 0]^{\mathrm{T}}$ m, $\mathbf{r}^{(2)} = [-0.5\ -0.5\ 0]^{\mathrm{T}}$ m, and $\mathbf{r}^{(3)} = [1.5\ 1.5\ 0]^{\mathrm{T}}$ m. To achieve the desired formation we have the following equations,

$$\bar{\rho}_d^{(1)} = [0\ 0\ 0]^{\mathrm{T}} \tag{69}$$

$$\bar{\rho}_d^{(2)} = [-\eta\ -\tau\ 0]^{\mathrm{T}} \tag{70}$$

$$\bar{\rho}_d^{(3)} = [\eta\ \tau\ 0]^{\mathrm{T}} \tag{71}$$

where $\eta = 1$ m is the longitudinal distance from the CM of the vehicle 1 to the CM of the other vehicles and $\tau = 1$ is the lateral distance between two neighboring vehicles. The variable $\bar{\rho}_d^{(i)}$ are the increment of the vehicle i in relation to the reference trajectory. The plot Figure in 7 shows how the vehicles converge to the desired triangular formation and that the real trajectories circumvent the obstacles without collisions.

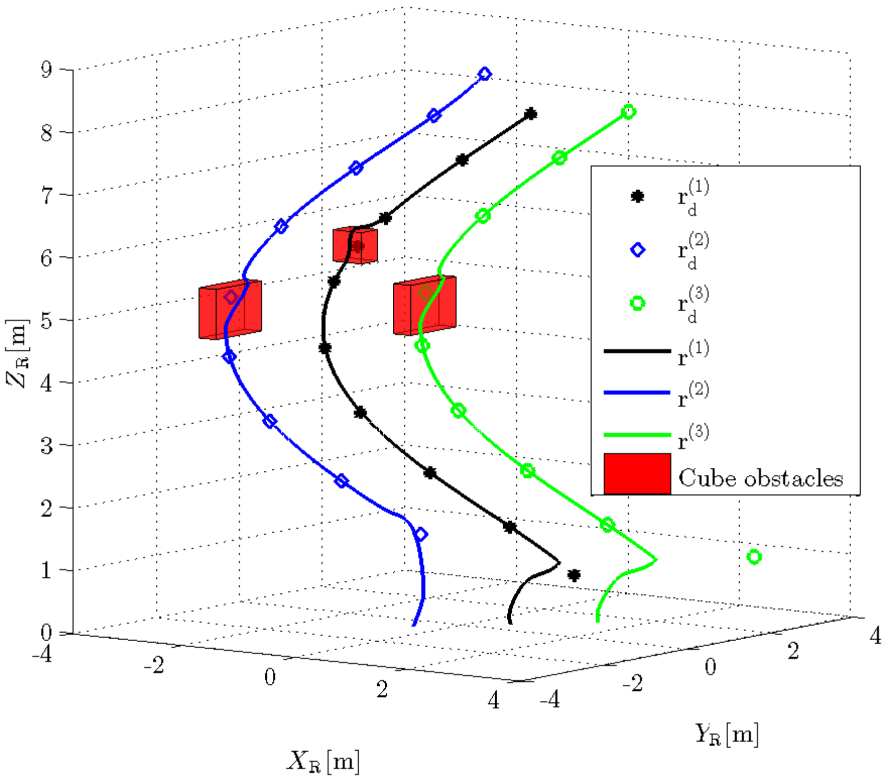

Figure 7. Formation control with obstacle avoidance

To better analyse the method, Figure 8 shows a 2D graphic, for all vehicles, considering that the obstacle is located in the inner reference trajectory. To validate that the obstacle avoidance requirement is attended, is showed the responses when the constraints in MPC are inactive and active, considering that a sustained disturbance force is applied on the system.

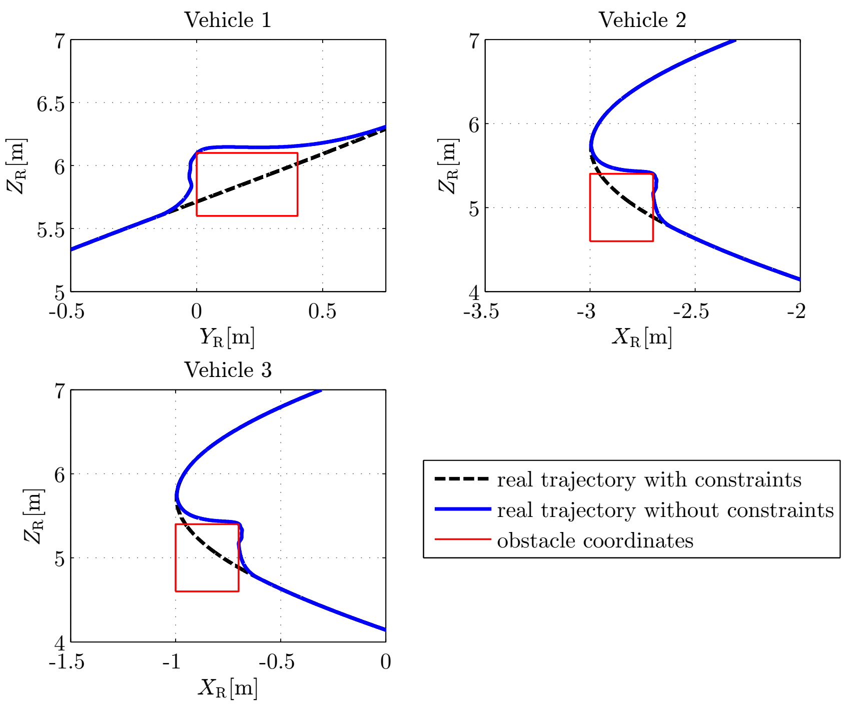

Figure 8. Obstacle avoidance acting in the three vehicles when undergoes disturbance.

It is observed that when constraints in MPC are active the controllers decides to change the trajectory of the vehicles to avoid the obstacles. While the vehicle 1 circumvent the obstacle in the plane YZ, the other two vehicles avoid the obstacles in the plane XZ. The disturbance force is imperceptible during the trajectory because the integral action provided by the incremental model, making the controllers able to reject the disturbance force. Note that the selection of the time-step length was appropriate once the incursions of the trajectory do not intersect the obstacles.

The Figures 9 and 10 shows the angle ϕ and the commanded force f_c for all vehicles of the formation, so that is possible to see that both constraints are respected. In the moment that the controllers change the trajectories to avoid the obstacle, an abrupt variation of ϕ and f_c occurs due to the high maneuverability and vertical accelerations that are demanded.

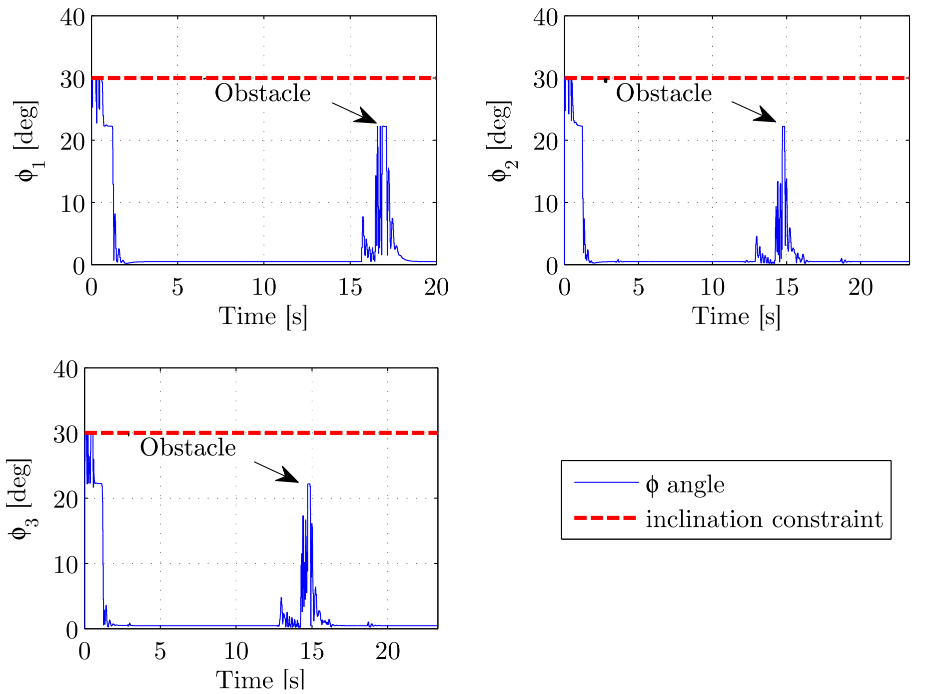

Figure 9. Inclination angle taking into account $\phi_{max} = 30^\circ$.

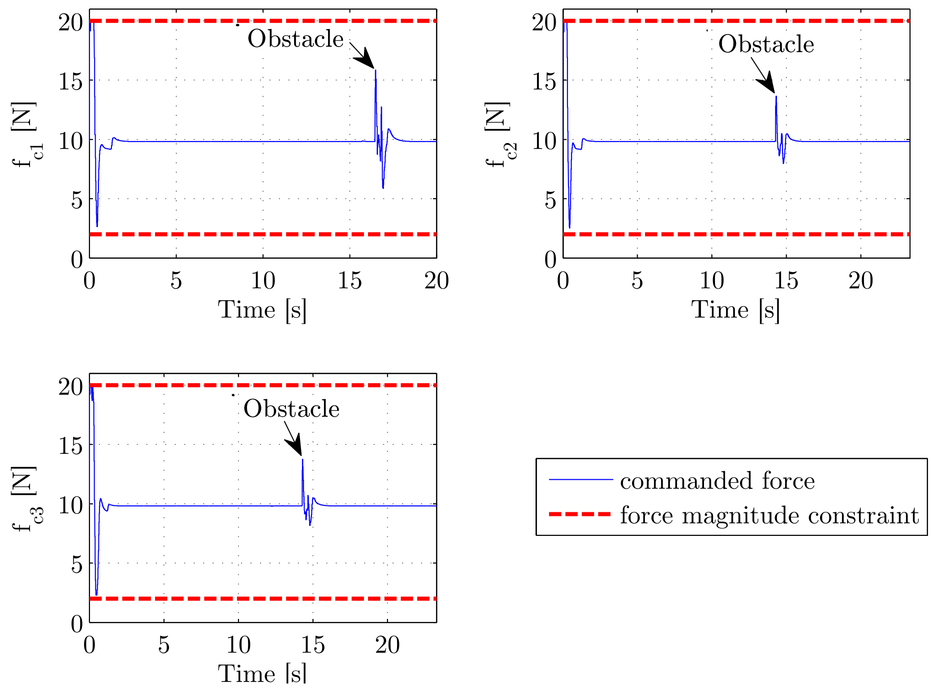

Figure 10. Total thrust magnitude graphics.

5. CONCLUSIONS

This article discussed the problem of adding position constraints to the formulation from a multirotor position control, so as to ensure obstacle and collision avoidance. The problem was solved using model predictive controllers with a formulation in a mixed-integer quadratic program (MIQP) form. The method was evaluated through computer simulations considering that the vehicle was subjected to disturbances forces to cause change in the formation while avoiding obstacles. It is concluded that the proposed method was able to control the multirotors formation in the presence of obstacles even under disturbance forces. The decentralized architecture was useful dealing with the MIQP scheme that requires larger computation capabilities. For a future work, obstacles moving in the space will be considered and a detection sphere of obstacles closest to the vehicle will be take into account in the optimization problem, with the proposal to have a more realistic application. Also, it is planned use a hardware-in-the-loop (HIL) environment for experimental evaluation of the proposed method.

6. ACKNOWLEDGEMENTS

The authors acknowledge the support of Conselho Nacional de Desenvolvimento Científico e Tecnológico (CNPq), by research project grant 475251/2013-0 and doctoral scholarship, and the Instituto Tecnológico de Aeronáutica (ITA) by the necessary support to realize the present work.

7. REFERENCES

Ailon, A., Arogeti, S. “Formation control strategies for autonomous quadrotor-type helicopters.” *IFAC Workshop on Research, Education and Development of Unmanned Aerial Systems.*, 2013.

Chao, Z., Ming, L., Shaolei, Z., Wenguang, Z. “Collision-free UAV Formation Flight Control based on Nonlinear MPC.” *Proc. AIAA Guidance, Navigation, and Control Conf.,* Honolulu, HI, 2008.

Kuwata, Y., How, J. “Real-time trajectory design for unmanned aerial vehicles using receding horizon control.” *M.S. thesis, Dept. Aeronautics Astronautics, Massachusetts Inst. Technol.*, Boston, 2003.

Maciejowski, J. M. “Predictive Control with Constraints.” *Harlow: Prentice-Hall* (2002)

Prado, I. A. A. , Santos, D. A. . “Multirotor position tracking using a linear constrained model predictive controller.” *22nd International Congress of Mechanical Engineering* (Ribeirão Preto, SP, 2013.)

Richards A. and How, J. P. “Aircraft trajectory planning with collision avoidance using mixed integer linear programming.” *American Control Conference* (2002)

Santos, D. A., Saotome, O. “Trajectory control of multirotor helicopters with thrust vector constraints.” *In: 2013 21st Mediterranean Conference on Control & Automation (MED) 2013* (Platanias. 21st Mediterranean Conference on Control and Automation, 2013. p. 375.)

Schouwenaars, T., Feron, E., How, J. “Multi-vehicle path planning for non-line of sight communication.” *Proceedings of the American Control Conference*, 2006.

Shuster, M. “A Survey of Attitude Representations.” *The Journal of the Astronautical Sciences* (41(4), 1993, 439-517)

Williams, H. P., Brailsford, S. C. “Computational Logic and Integer Programming.” *Advances in Linear and Integer Programming,* edited by J. E. Beasley, Clarendon, Oxford, 249-281, 1996.

8. RESPONSIBILITY NOTICE